Journal of Ambient Intelligence and Humanized Computing
https://doi.org/10.1007/s12652-020-02204-7

ORIGINAL RESEARCH

A precise feature extraction method for shock wave signal with improved CEEMD-HHT

Zonglei Mou[1] · **Xueben Niu**[1] · **Chen Wang**[1]

Received: 2 March 2020 / Accepted: 6 June 2020

Abstract
Efficient extraction of feature parameters is the key to evaluating weapon damage performance. At present, many classical feature extraction algorithms have the problem that the extraction cannot meet the actual needs. A precise feature extraction method based on improved complementary ensemble empirical mode decomposition (CEEMD) with Hilbert-Huang Transform (HHT) was proposed in this paper to solve problems such as large noise and difficulties in extracting features of shockwave overpressure signals in complex test environment. We introduced CEEMD to decompose original explosion shockwave signals and adopted wavelet packet threshold de-noising to extract useful information from noisy high-frequency intrinsic mode functions (IMFs). The correlation coefficient algorithm is introduced to remove unrelated IMFs. In addition, we performed reconstruction of original signals to extract true time-course feature and utilized Hilbert-Huang Transform (HHT) to achieve precise extraction of instantaneous feature and energy spectrum of the various IMFs. The improved CEEMD-HHT is a precise method for shock wave signal analysis. It not only effectively removes noise, but also retains effective high-frequency information without losing useful information. Additionally, it overcomes the problems of mode mixing in empirical mode decomposition (EMD), and has the advantages of feature extraction with high accuracy and self-adaptation. The effectiveness of the proposed method is demonstrated by 2 groups of experimental data, and it precisely extracts instantaneous feature and energy spectrum of shockwave overpressure signal, which provide new theoretical basis for the evaluation of weapon damage.

Keywords Improved CEEMD · HHT · Shockwave overpressure · Feature extraction · Energy spectrum

1 Introduction

In order to more accurately evaluate weapon damage performance, the extraction of characteristic parameters is actually a very important link. The extraction of feature parameters is directly related to the accuracy of damage performance evaluation (Alonso et al. 2006; Wang et al. 2010). The explosion shockwave overpressure test usually takes place in complex environments and the test data often contains lots of noise due to the complex electromagnetic interference, fragment impact and ground vibration caused by explosion. Therefore, it is of great significance to select a reasonable de-noising and feature extraction method to extract effective shockwave overpressure feature parameters from the measured noise-containing signals (Li et al. 2017). Considering the importance of noise reduction and feature extraction of shockwave overpressure signals, many scholars have carried out related researches and made some achievements. Currently, commonly used de-noising methods for shockwave overpressure signals include low-pass filtering, wavelet transform de-noising and EMD noise reduction.

Xu et al. (2003) comparatively studied the de-noising effects wavelet transform and some other de-noising methods for shockwave overpressure signals. Daubechies and Symlets wavelet families are compared in threshold treating of shock wave data, and they proposed some instructive suggestions on noise reduction of shockwave overpressure signals. Yao et al. (2017) combined EMD with adaptive least squares (ALS) to improve the dynamic calibration accuracy of pressure sensors. By identifying and excluding those components involved in noises, the noise-free output could be reconstructed with the useful frequency modulations.

✉ Zonglei Mou
mzlsdut@163.com

[1] College of Electrical Engineering and Automation, Shandong University of Science and Technology, Qingdao 266590, People's Republic of China

Published online: 13 June 2020

Experimental results show that the proposed method works well in reducing the influence of noise and yields an appropriate mathematical model. Du et al. (2010) applied a low-pass filter, a wavelet transform and other methods to de-noise the measured shock wave signal. They compared the advantages and disadvantages of these methods and suggested some various methods in which to reduce the noise from shock wave signal. Related feature extraction methods (Ma et al. 2020; Al-Ayyoub et al. 2017; Birajdar et al. 2019; Li et al. 2018) are used in multiple fields. After feature extraction, various machine learning algorithms(Qian et al. 2015, 2016, 2017; Xia et al. 2019a, b; Qian et al. 2018a, b; Xue et al. 2017, 2018a, b) are needed to achieve final recognition and inspection.

Currently, there are many researches on the time domain or frequency domain of shockwave overpressure signals and few researches on their instantaneous features (instantaneous frequency and instantaneous amplitude) and energy spectrum (Li et al. 2017). Feature parameters used to evaluate shockwave overpressure damage performance mainly include peak overpressure, positive pressure duration and specific impulse. Conventional feature extraction methods for time domain and frequency domain include short-time Fourier transform (STFT) and wavelet transform. Li et al. (2009) analyzed the non-linear and non-stationary shock signal with HHT, and gave the marginal spectrum compared to the Fourier frequency spectrum. After filtering and de-noising the original signals with wavelet packet transform, Li et al. (2017) adopted EMD to adaptively decompose the filtered signals and extract effective IMFs. Warhead damage performance was evaluated from the perspective of energy spectrum.

Although these signal de-noising and feature extraction methods realize noise reduction and feature extraction of shockwave overpressure signals in different ways, there are still some problems with them in complex test environments. For instance, although EMD adaptively and successively decomposes signals from high frequency to low frequency and preserves signal features in the decomposition process, it is not suitable for instantaneous non-stationary signals. Furthermore, EMD itself has a serious drawback, namely, the mode mixing problem (Wu et al. 2009; Yeh et al. 2010).

CEEMD is a significant improvement of ensemble empirical mode decomposition (EEMD). It not only retains advantages of EMD in processing non-stationary signals, but also effectively avoids mode mixing of EMD (Li et al. 2015). However, de-noising and feature extraction methods directly discarding high-frequency IMFs which obtained via CEEMD may lose effective information of high-frequency element. Therefore, a more effective method is needed to de-noising and extract clean feature information of signals.

To address the above shortcomings, we propose an adaptive de-noising and precise feature extraction method based on improved CEEMD-HHT. This feature extraction method combines the ideas of CEEMD and HHT algorithms. Compared with traditional EMD, the algorithm can not only effectively remove noise but also retain high-frequency overpressure data. Compared with HHT alone, the proposed algorithm can more accurately evaluate the warhead damage. The main contributions of this paper can be outlined as follows:

1. We proposed an adaptive de-noising method for shockwave overpressure signals based on improved CEEMD. This algorithm solves the problems of mode mixing in EMD and retains high-frequency overpressure data while effectively eliminating noise, thereby exhibiting the advantages of multi-resolution and self-adaptation.
2. We proposed an HHT-based precise extraction method for instantaneous features and energy spectrum of shockwave overpressure signals, thereby providing new theoretical basis for the precise evaluation of warhead damage performance.

The paper is structured as follows: Chapter 2 describes relevant theoretical basis of the algorithm. Chapter 3 introduces the precise extraction method for instantaneous feature and energy spectrum of shockwave overpressure signals. Chapter 4 demonstrates test verification and data analysis. Chapter 5 is the conclusion part.

2 Theoretical analysis of the algorithm

2.1 CEEMD

EEMD (Xue et al. 2015) can separate the high-frequency noise from the original signal via adding the white noise, but the low-frequency noise cannot be reduced. CEEMD is an improved algorithm based on EMD (He et al. 2019).

Suppose that $x(n)$ is the original signal of the discrete number n, $E_j(\cdot)$ is the jth intrinsic mode function (IMF) of the signal after EMD decomposition, $\omega^i(n)(i = 1, \cdots, I)$ is the white Gaussian noise with the unit variance of zero and ε_k is ratio of the signal to noise in each order. Decomposition steps of improved CEEMD are as follows:

Step 1: add white noise to the signal, decompose the signal by EMD for i times ($i = 1, 2 \cdots, I$) and take the average of the first-order IMF_1^i, thereby obtaining the first intrinsic mode function:

$$IMF_1(n) = \frac{1}{I}\sum_{i=1}^{I} IMF_1^i(n) \tag{1}$$

Step 2: calculate the remainder $r_1(n)$, when k = 1

$$r_1(n) = x(n) - IMF_1(n) \tag{2}$$

Step 3: add white noise to the first-order remainder $r_1(n)$ to constitute a new signal:$r_1(n) + \varepsilon_1 E_1\left(\omega^i(n)\right)$, perform EMD decomposition on the new signal and take the average, thereby obtaining the second intrinsic mode function:

$$IMF_2(n) = \frac{1}{I}\sum_{i=1}^{I} E_1\left(r_1(n) + \varepsilon_1 E_1\left(\omega^i(n)\right)\right) \tag{3}$$

Step 4: calculate the Kth-order remainder $r_k(n)$:

$$r_k(n) = r_{k-1}(n) - IMF_k(n) \tag{4}$$

Step 5: add white noise to the kth-order remainder $r_k(n)$ to constitute a new signal $r_k(n) + \varepsilon_k E_k\left(\omega^i(n)\right)$, perform EMD decomposition on the new signal and take the average, thereby obtaining the (k + 1)th intrinsic mode function:

$$IMF_{k+1}(n) = \frac{1}{I}\sum_{i=1}^{I} E_1\left(r_k(n) + \varepsilon_k E_k\left(\omega^k(n)\right)\right) \tag{5}$$

Step 6: end the decomposition when there is only one extreme point in the remainder. Otherwise, return to Step 4 to continue the iteration until the termination conditions are met, thereby obtaining the final remainder $R(n)$.

$$R(n) = x(n) - \sum_{k=1}^{K} IMF_k \tag{6}$$

The original signals after de-noising and reconstruction can be expressed as:

$$x(n) = \sum_{k=1}^{K} IMF_k + R(n) \tag{7}$$

K represents the total number of IMFs obtained. Formula (7) shows that CEEMD is a complete decomposition method that can precisely reconstruct original signals with IMFs and the residual function.

2.2 Selection principles of effective IMFs

Not all IMFs obtained through CEEMD decomposition correctly represent feature information of original signals. The extraction of effective IMFs is an important part of noise reduction, reconstruction and feature extraction. Theoretically, higher correlation between original signal and IMFs corresponds to a larger number of effective signal components. Therefore, we introduce the correlation coefficient criteria to extract effective IMFs.

Suppose that the correlation coefficient (Yang et al. 2017) between the ith IMF C_i and the original signal x is r_i. The following conclusion can be drawn on the basis of the definition of correlation coefficient (Li et al. 2017):

$$r_i = \frac{\sum\left(c_i - \overline{c_i}\right)\left(x - \overline{x}\right)}{\sqrt{\sum\left(c_i - \overline{c_i}\right)^2 \sum\left(x - \overline{x}\right)^2}} \tag{8}$$

In this paper, IMFs are selected in accordance with the following principles: eliminate ineffective high-frequency IMFs that contain lots of noise; de-noise high-frequency IMFs that contain a small amount of noise by wavelet packet transform, thereby reconstructing new IMFs; directly extract features of highly correlated low-frequency IMFs.

2.3 Wavelet packet threshold de-noising

The wavelet packet algorithm is a further and detailed decomposition of high-frequency information obtained through wavelet transform (Shucong et al. 2016). Wavelet packet decomposition decomposes the signal $x(t)$ into the linear superposition of spatial basis function systems $\left\{b_\lambda(t)\right\}$. The following conclusion can be drawn when the signal is projected onto different spaces:

$$x(t) = \sum_{\lambda\in\Lambda} c_\lambda b_\lambda(t) \tag{9}$$

It is feasible to de-noise the original signal by processing coefficient c_λ and obtain the feature information. Suppose that $x(t)$ is the space function on $L^2(R)$. When the discrete sampling sequence $\{x(p)\}_{p=1,2,\cdots,N}$ is decomposed, the wavelet packet decomposition algorithm can be expressed as:

$$\begin{cases} C_p^{j,2n} = \sum_k h(k-2p) C_k^{j+1,n} \\ C_p^{j,2n+1} = \sum_k g(k-2p) C_k^{j+1,n} \end{cases} \tag{10}$$

According to formula (10), wavelet packet decomposition decomposes signal into different frequency bands through the linear combination of high-pass and low-pass conjugate quadrature filters h and g, thereby eliminating invalid frequency bands and realizing the purpose of de-noising. Wavelet packet threshold de-noising is mainly influenced by wavelet basis and threshold selection. Wherein, the threshold consists of hard threshold and soft threshold. Soft threshold de-noising(Guo et al. 2018), which achieves optimal threshold estimation and guarantees smoothness of the reconstructed signals after de-noising, is expressed as:

$$d_j' = \begin{cases} 0 & \left|d_j\right| < \lambda_j \\ sign\left(d_j\right)\left(\left|d_j\right| - \lambda_j\right) & \left|d_j\right| \geq \lambda_j \end{cases} \tag{11}$$

where d_j' is the soft threshold signal of the signal d_j, and λ_j is the threshold value, respectively.

2.4 CEEMD-wavelet packet threshold de-noising

The noisy explosion shockwave signal $x(t)$ after adaptive decomposition by CEEMD can be expressed as:

$$x(t) = \sum_{i=1}^{n} IMF_i(t) + R_n(t) \tag{12}$$

where $IMF_i(t)$ is the intrinsic mode function,$R_n(t)$ is the remainder, and n is the number of intrinsic mode functions when $R_n(t)$ is sufficiently small or has only one extreme value.

We used correlation coefficient to determine the correlation between IMFs and original signal. For effective IMFs that contain noise, wavelet packet transform de-noising was employed to extract useful information from IMFs, thereby reconstructing new IMFs. Finally, the shockwave signal can be reconstructed by summing effective low-frequency IMFs without noise and effective high-frequency IMFs reconstructed through wavelet packet transform.

The reconstructed signal after de-noising can be expressed as:

$$\tilde{x}(t) = \sum_{i=1}^{n} c_i'(t) + \sum_{i=n+1}^{m} c_i(t) + R_n(t) \tag{13}$$

where $\tilde{x}(t)$ is the signal reconstructed after de-noising, $c_i'(t)$ represents IMFs reconstructed through wavelet packet threshold de-noising, $c_i(t)$ represents IMFs without wavelet packet threshold de-noising, and $R_n(t)$ is the residual function.

3 Feature extraction of explosion shockwave signals

Due to the instantaneity and non-stationarity of explosion shockwave signal, it is particularly important to research time-course features, spectrum characteristics and instantaneous features of signals. In addition, it has been previously established that the energy spectrum is an effective feature by which to characterize a blast wave. The higher the energy spectra in a frequency band of a shockwave overpressure, the greater the damage to a target in the same frequency band shall be, which has been proved in many studies (Li et al. 2017). To evaluate warhead damage performance more accurately, it is necessary to precisely extract energy spectrum of explosion shockwave signals. After extracting effective information from the original signals by adaptive de-noising, we emphatically explored methods of extracting energy spectrum of explosion shockwave overpressure signals.

3.1 Extraction of time-course features

The original signals can reproduce real time attenuation curves of shockwave overpressure after adaptive de-noising and reconstruction, thereby precisely extracting feature parameters such as peak overpressure, positive pressure duration and specific impulse. It provides accurate data for the evaluation of weapon damage performance.

3.2 Extraction of energy spectrum

HHT was applied to IMFs reconstructed by wavelet packet threshold de-noising and low-frequency IMFs obtained through adaptive decomposition. The instantaneous frequency spectrum of the various IMFs can be obtained through HHT (Li et al. 2015). The original signal is decomposed into a series of components:c_1, c_2 …, c_n, and the remainder r_n. The original signal $x(n)$ can be reconstruct as:

$$x(n) = \sum_{i=1}^{n} c_i + r_n \tag{14}$$

The Hilbert transform of $x(n)$ is defined as the convolution of $x(n)$ and $\frac{1}{\pi n}$:

$$H[x(n)] = x(n) \otimes \frac{1}{\pi n} \tag{15}$$

Therefore, for an arbitrary signal $x(n)$, its Hilbert transform (Xu et al. 2020)can be defined as

$$y_i(i) = c_i(i) + jH\left[c_i(i)\right] = a(i)e^{j\phi(i)} \tag{16}$$

The amplitude function $a(t)$, phase function $\phi(t)$ and instantaneous frequency $\omega(t)$ are expressed as follows, respectively:

$$\begin{cases} a(t) = \sqrt{c^2(t) + H^2[c(t)]} \\ \phi(t) = \arctan \dfrac{H[c(t)]}{c(t)} \\ \omega(t) = \dfrac{d\phi(t)}{d(t)} \end{cases} \tag{17}$$

Therefore, each IMF can be calculated through HHT, and the signal $x(n)$ can be expressed as:

$$x(t) = \sum_{i=1}^{n} a_i(t) \exp\left(j \int \omega_i(t) dt\right) \tag{18}$$

Furthermore, the Hilbert spectrum $h(\omega, t)$ of the original can be obtained through integral calculation of $x(\omega, t)$, which can be expressed as,

$$h(\omega) = \int_0^T H(\omega, t)dt = \sum_{i=1}^{n} \int_0^T \mathrm{Re}\left(a_i(t)e^{j\int \omega_i(t)dt}\right)dt \quad (19)$$

In the end, the energy spectrum can be obtained by calculating time integral of the square of the Hilbert spectrum (Li et al. 2016) amplitude of the signal $x(t)$:

$$ES(\omega) = \int_0^T x^2(\omega, t)dt \quad (20)$$

The energy spectrum presents energy equations of each frequency component, and it also represents the energy accumulated by each frequency component over the time t. It clearly and specifically demonstrates the distribution of energy with frequency.

4 Experimental analysis

4.1 Test environment and data acquisition

A set of blast wave experiments was designed to study feature parameters of explosion shockwave signals. The test nodes (1–8) were placed in two fiber links in turn along the explosion area including 3.5 m, 4 m, 6 m and 8 m. Theoretically, the test nodes at the same distance from the blaster center in each link have the similar information in static blast experiment. Therefore, 4 test nodes in one link were randomly selected, which were denoted as case 1 to case 8, respectively. First group, a set of explosion shockwave experiments was designed consisting of 4 test nodes, which are denoted as cases 1–4, respectively. In these cases, the explosion shockwave was generated from the explosion of 2Kg TNT explosive equivalence. The second group, the test nodes were at the same distance with the explosion of 4Kg TNT explosive equivalence, which are denoted as cases 5–8, respectively. During the test, the warheads were positioned on the top of a wooden platform 1.5 m above the ground.

Layout of the shockwave overpressure test system based on a distributed optical fiber network is shown in Fig. 1. The test system was mainly composed of shockwave overpressure test nodes, gateway node, control terminal, and distributed optical fibers for communication. All test nodes were placed in the electromagnetic shell and then placed in the soil. Only the sensitive surface of the pressure sensors exposed to the ground to capture the blast wave signal. In addition, all nodes in the test system communicated over a distributed fiber-optic LAN.

The experiment produced a total of 8 shockwave pressure signals. Time-domain waveforms of the explosion shockwave signal in case 7 were used as a random sample, as shown in Fig. 2a. As the figure shows, explosion shockwave signal was characterized by steep rising edge, sudden changes and short duration, so that it is a typical

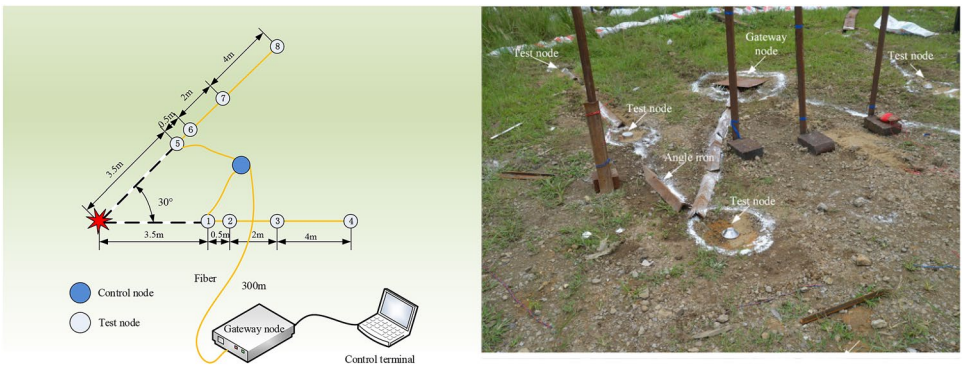

Fig. 1 The site layout of the test system

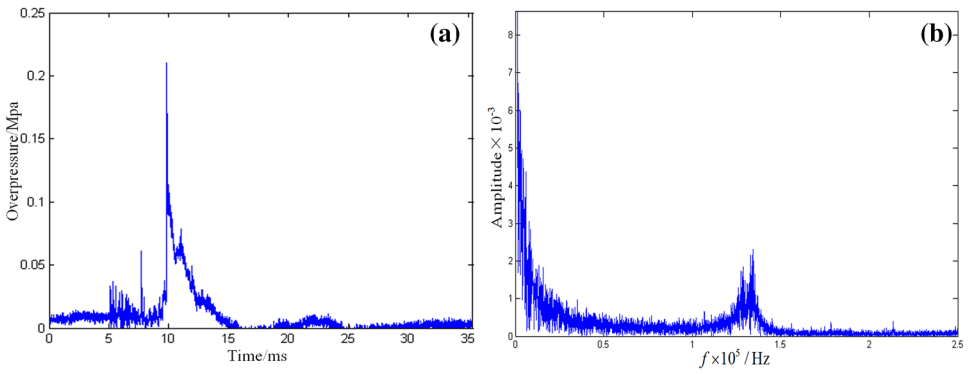

Fig. 2 The measured shock wave and the spectrogram: **a** A typical record of shockwave overpressure; **b** Spectrogram of shockwave overpressure

instantaneous non-stationary signal. As Fig. 2b (frequency spectrum of the signal) shows, explosion shockwave signal has rich frequency spectrum, which is manifested as multiple bands and multiple peaks. Shockwave signals generated by warhead explosion, whose frequency is smaller than 30 kHz, is significantly influenced by strong noise between 100 and 150 kHz. The presence of strong noise seriously affects the interpretation of overpressure information and the extraction of feature parameters. Therefore, there is a need for effective de-noising method.

4.2 Adaptive de-noising method based on improved CEEMD

We employed CEEMD to adaptively decompose the measured shockwave overpressure signal. The IMFs and remainder obtained are shown in Fig. 3.

In Fig. 3, IMF1-IMF3 are high-frequency components decomposed from the original signal. As the number of decomposition increases, the frequency of the various components gradually decreases until the final remainder R13 is obtained. With the correlation coefficient algorithm, IMF1-IMF3 enjoy high frequency and low correlation, which indicates that they are high-frequency noisy IMFs. IMF4-IMF7 are high-frequency elements that contain a certain amount of noise, thereby needing to be de-noised and reconstructed to extract effective high-frequency information. IMF8-IMF12 are dominant frequency sub-bands of the signal, and R13 is the remainder. Here, the wavelet packet threshold denoising method is only used for noise reduction of IMF4-IMF7. Finally, the reconstructed signal after de-noising is shown in Fig. 4.

It can be seen from Fig. 4 that the adaptive de-noising algorithm based on improved CEEMD effectively eliminates noise and retains high-frequency overpressure information. It eliminates noise more thoroughly, thereby being more suitable for analyzing and filtering of mutational signal and instantaneous non-stationary signal. According to the reconstructed signal after de-noising, peak overpressure and positive pressure duration in case 7 are 0.187MP and 12.127 ms separately. It offers a good solution to noise reduction and information extraction of explosion shockwave signals.

4.3 Extraction of instantaneous features

After extracting effective IMFs, we adopted HHT to extract instantaneous features of IMFs and listed corresponding Hilbert-Huang spectrum in Fig. 5. Due to the limited space, we merely list the Hilbert-Huang spectrum in case 7. Hilbert-Huang spectrum in other cases can be obtained in the same way.

It can be seen from Fig. 5 that the instantaneous features extraction method based on HHT precisely extracts instantaneous features of shockwave overpressure signals, which perfectly demonstrates time–frequency-amplitude variations of the shockwave overpressure signals.

4.4 Extraction of energy spectrum

Energy spectrums of shockwave signals in cases 1–8 were extracted and analyzed in accordance with the proposed method. Percentage distribution of energy spectrum in cases 1–8 were obtained through the normalization of corresponding explosion shockwaves, as shown in Fig. 6a, b. Shockwave energy in the 8 cases and energy distribution of each frequency band are shown in Table 1.

According to the comparative analysis of Fig. 6 and Table 1, the following conclusions can be drawn: total energy of explosion shockwave signals generated by the same kinds of explosives decreases with the distance increase from explosion site. In addition, the energy in high-frequency bands attenuates rapidly while that in low-frequency bands attenuates slowly and has a long duration. Therefore, shockwave signals have a wider range of damage at low frequencies.

Here, we divided the frequency into multiple frequency bands to demonstrate the distribution of energy in each frequency band more intuitively and vividly. The distribution of energy spectrum was represented with energy histograms in each frequency band. Figures 7a–d are energy histograms of explosion shockwave signals generated by warheads with the explosive weight of 2Kg at 4 different distances (cases 1 to 4).

Figures 8a–d are energy histograms of explosion shockwave signals generated by warheads with the explosive weight of 4 Kg at 4 different distances (cases 5–8).

Figures 7, 8 show that shockwave energy is mainly concentrated in the low-frequency band of 0–500 Hz. In other words, energy in low-frequency bands is significantly larger than that in high-frequency bands.

Effectiveness of the HHT-based feature extraction method was verified by the analytical results of instantaneous features and energy spectrums of explosion shockwave signals. In addition, the significant attenuation and distribution laws of shockwave overpressure energy spectrums were obtained. Under these laws, it is feasible to realize high-frequency and low-frequency energy distribution of different explosion shockwaves, thereby achieving different damage effects.

5 Conclusions

An adaptive de-noising and precise feature extraction method based on improved CEEMD-HHT was proposed in this paper. The adaptive de-noising algorithm based on improved CEEMD not only eliminates noise efficiently,

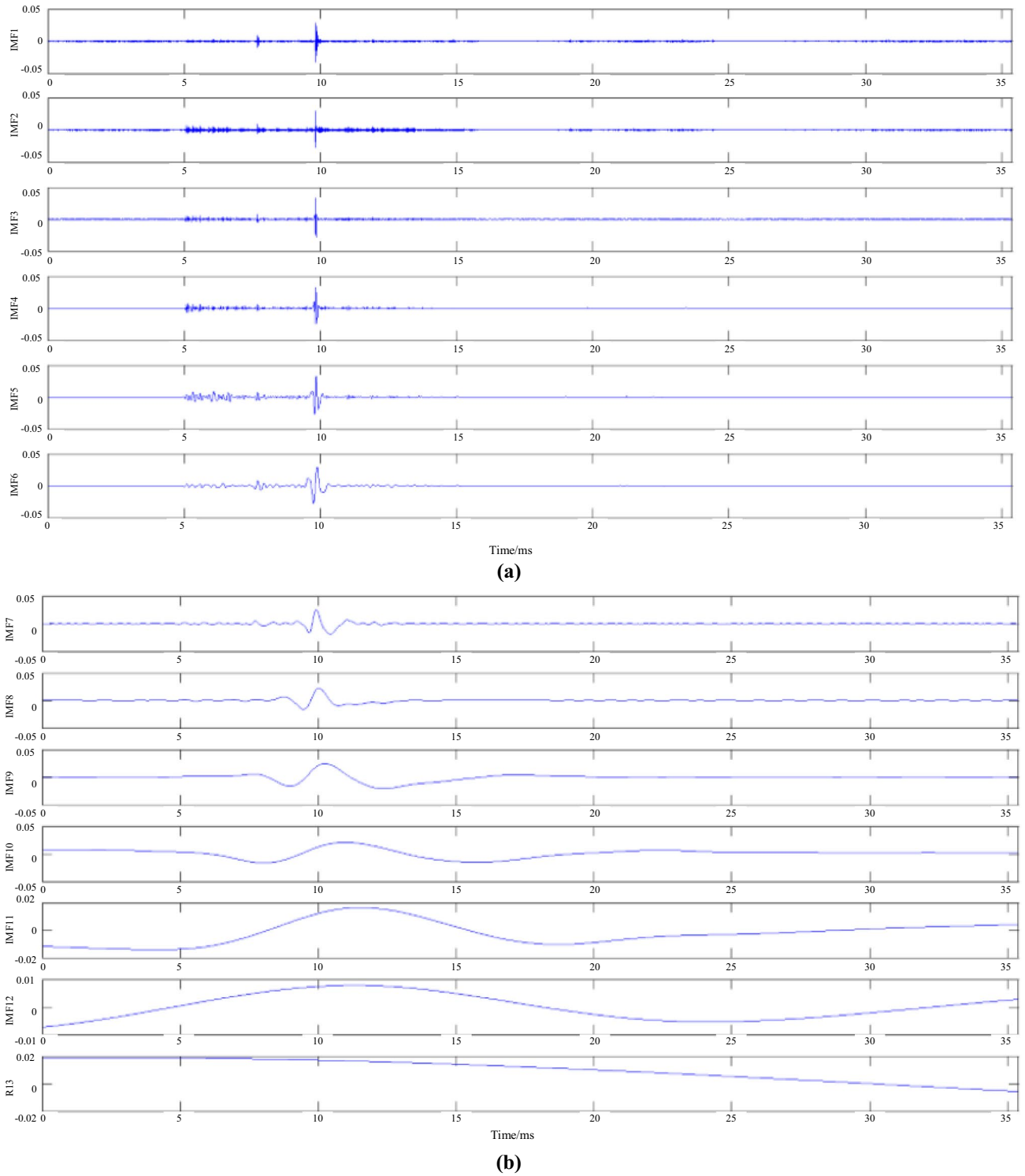

Fig. 3 The decomposition results via CEEMD: **a** IMF1 ~ IMF6; **b** IMF7 ~ IMF12 and the remainder R13

but also retains effective high-frequency information while solving the problems of energy leakage caused by wavelet packet de-noising and mode mixing of EMD, thereby exhibiting the advantages of multi-resolution and self-adaption. We performed HHT over low-frequency IMFs obtained through adaptive de-nosing and high-frequency IMFs reconstructed through wavelet packet transform to precisely extract instantaneous features and energy

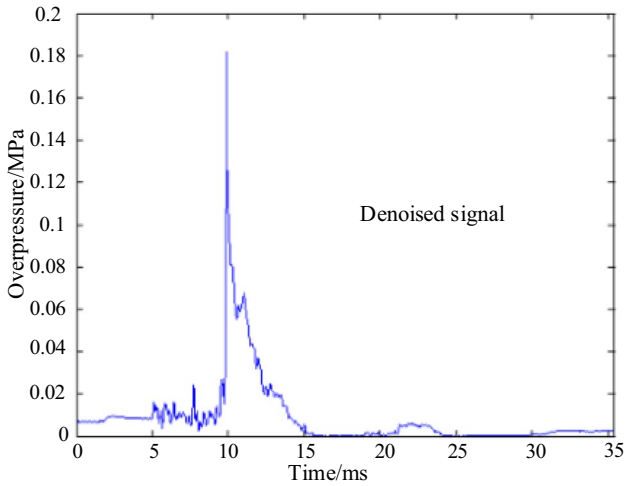

Fig. 4 The reconstructed signal after de-noising

spectrum of shockwave overpressure signals, thereby further improving the weapon damage performance evaluation system. Effectiveness of the proposed method was proved by the de-noising effects and the feature extraction results of the test data, which provides new theoretical basis for the evaluation of weapon damage performance. Although the proposed feature extraction method can effectively retain high-frequency information and avoid the problem of energy leakage. This method increases the computational complexity of the algorithm to a certain extent and improves the running time of the algorithm. This is where the research needs to be further optimized in the future.

Fig. 5 The Hilbert-Huang spectrum

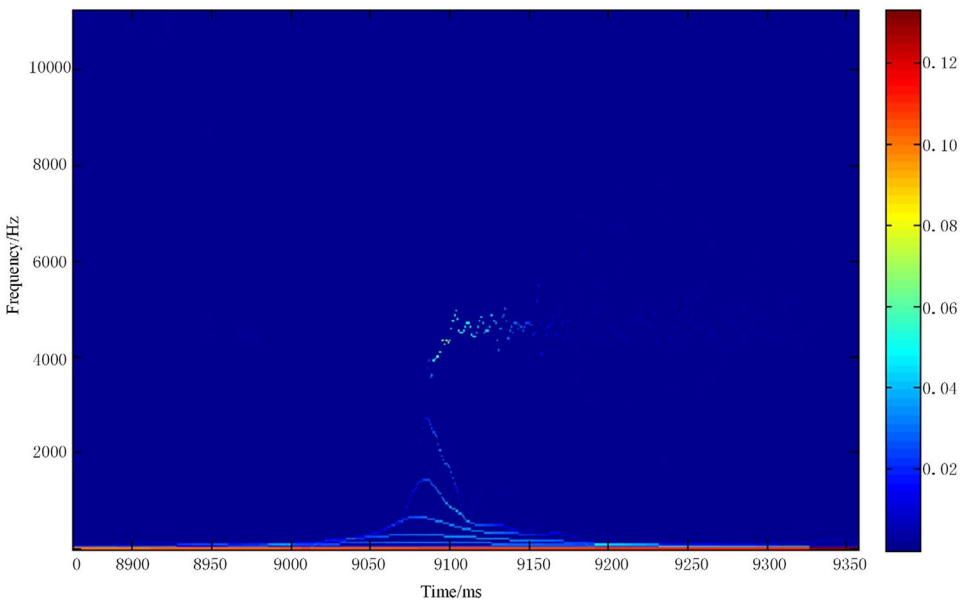

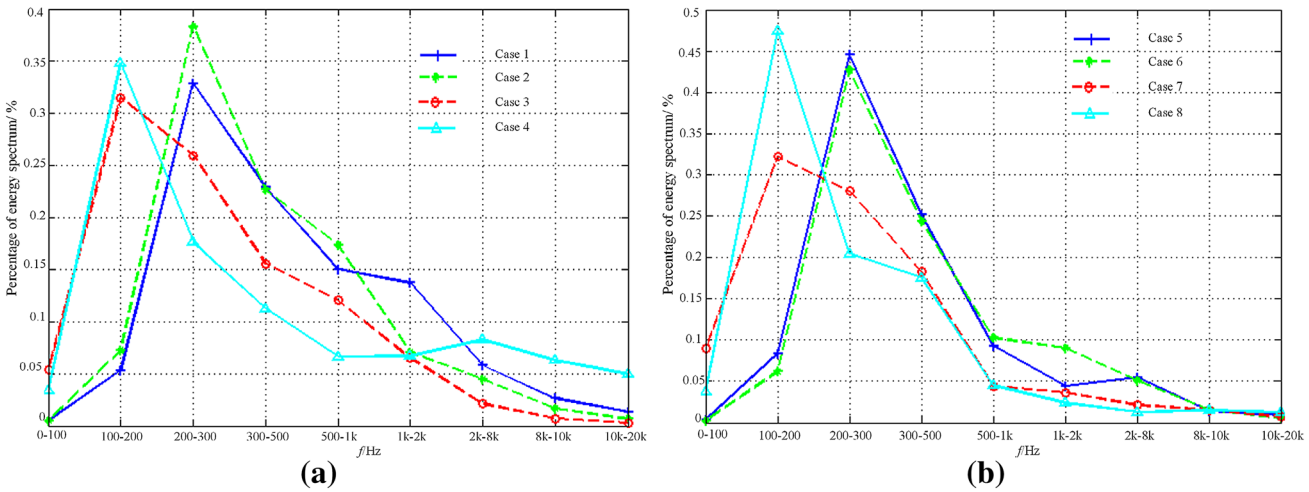

Fig. 6 Energy spectrums of shockwave signals: **a** cases 1–4; **b** cases 5 to 8

Table 1 Energy distributions of the shock wave signals in different frequency bands

f/Hz	Energy distribution							
	Case 1	Case 2	Case 3	Case 4	Case 5	Case 6	Case 7	Case 8
0–100	0.238	0.221	0.515	0.061	0.513	0.291	1.320	0.182
100–200	2.550	3.340	3.040	0.619	12.100	8.350	4.700	2.310
200–300	15.700	17.600	2.499	0.313	64.000	57.400	4.080	0.995
300–500	10.900	10.400	1.500	0.119	36.100	32.800	2.670	0.856
500–1 k	7.190	7.990	1.161	0.118	13.339	13.800	0.644	0.221
1–2 k	6.570	3.270	0.637	0.119	6.330	12.100	0.529	0.115
2–8 k	2.780	2.060	0.202	0.148	7.870	6.830	0.315	0.063
8–10 k	1.260	0.764	0.067	0.112	2.071	2.140	0.229	0.071
10–20 k	0.644	0.312	0.026	0.087	1.370	0.781	0.101	0.062
Total energy(E)	47.832	45.957	9.647	1.696	143.693	134.492	14.588	4.875

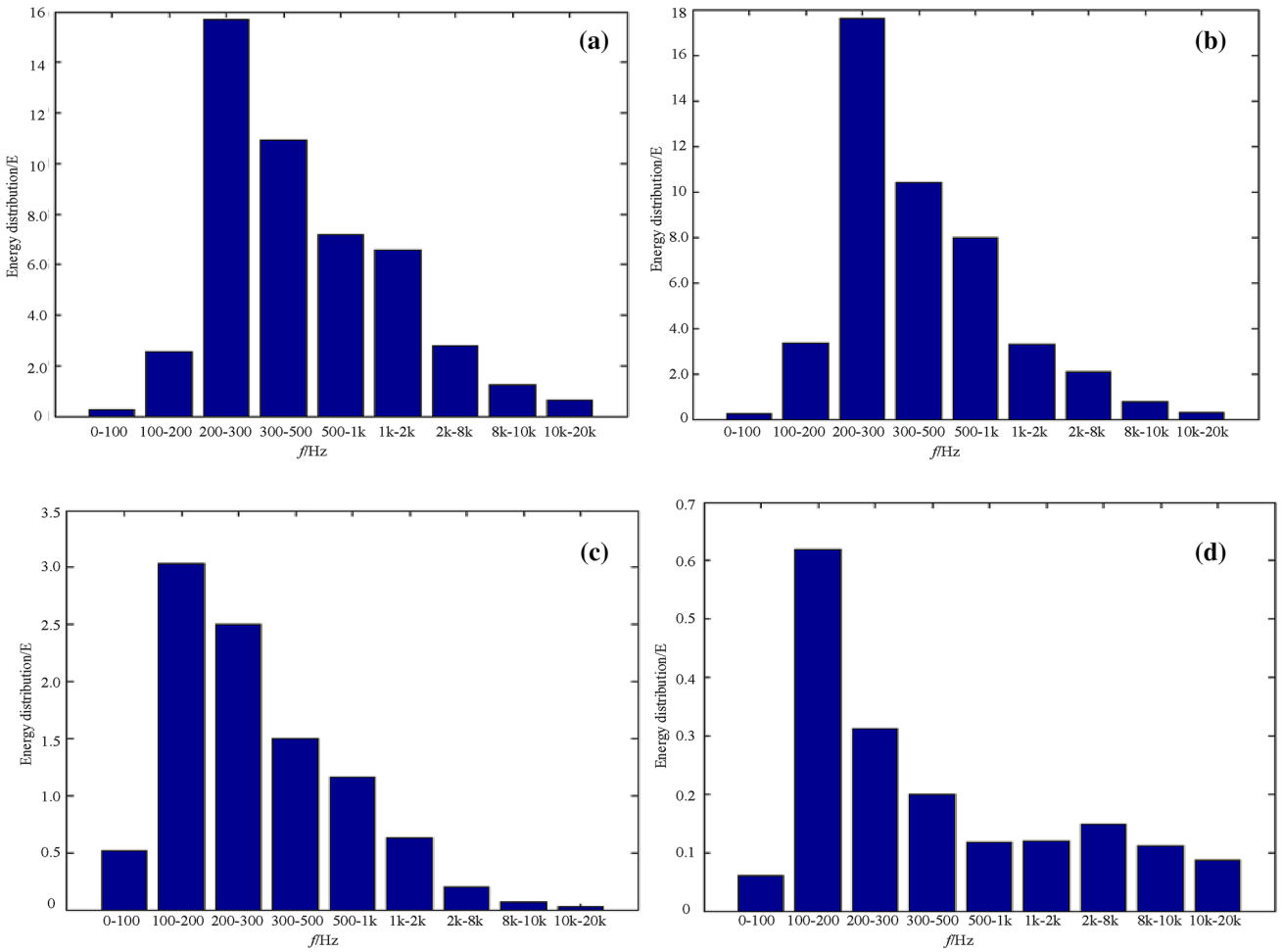

Fig. 7 Energy histograms of shockwave signals: **a** case 1; **b** case 2; **c** case 3; **d** case 4

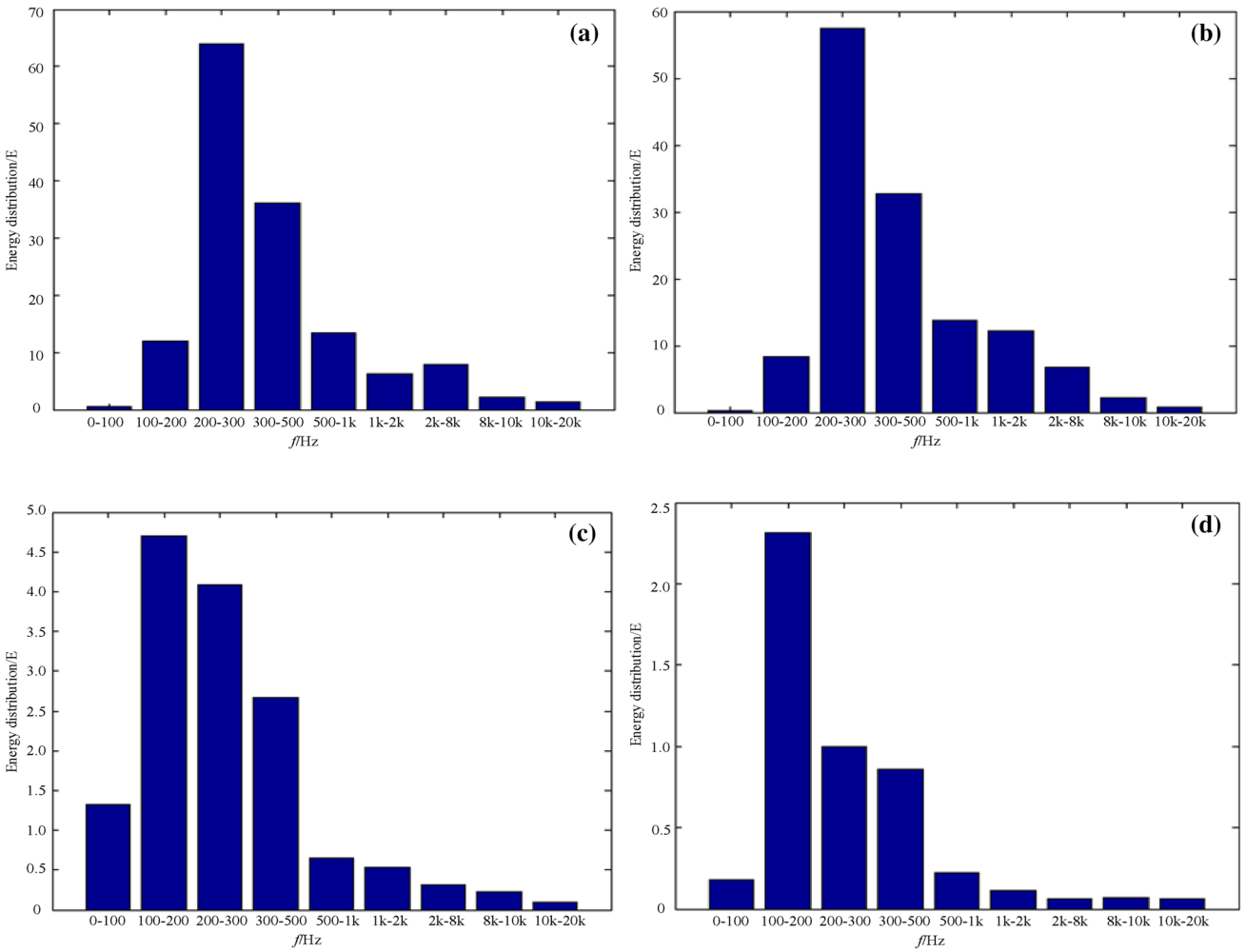

Fig. 8 Energy histograms of shockwave signals: **a** case 5; **b** case 6; **c** case 7; **d** case 8

Acknowledgements This work was supported by the National Defense Basic Scientific Research of China under Grant No. JCKY2019208A007 and Key Laboratory for Robot and Intelligent Technology of Shandong Province under Grant No. KLRIT2018005.

Compliance with ethical standards

Conflict of interest The authors declare that there is no conflict of interests regarding the publication of this paper.

References

Al-Ayyoub M, Jararweh Y, Rabab'ah A, Aldwairi M (2017) Feature extraction and selection for Arabic tweets authorship authentication. J Ambient Intell Hum Comput 8(3):383–393

Alonso FD, Ferradás EG, Pérez JFS et al (2006) Characteristic overpressure–impulse–distance curves for the detonation of explosives, pyrotechnics or unstable substances[J]. J Loss Prev Process Ind 19(6):724–728

Birajdar GK, Patil MD (2019) Speech/music classification using visual and spectral chromagram features. J Ambient Intell Hum Comput

Du H, Zu J (2010) Digital signal processing method to air blast shock wave[C]//2010 2nd international conference on information engineering and computer science. IEEE, 1–4.

Guo X, Sun C, Wang P et al (2018) Hybrid methods for MEMS gyro signal noise reduction with fast convergence rate and small steady-state error[J]. Sens Actuators A 269:145–159

He M, Feng L, Qu J (2019) Denoising algorithm of Φ_OTDR signal based on clear iterative EMD interval-thresholding[J]. Opt Commun 453:124352

Li W, Yuan W-Q (2018) Multiple palm features extraction method based on vein and palmprint. J Ambient Intell Hum Comput. https://doi.org/10.1007/s12652-018-0699-1

Li M, Liu M, Bai L (2009) Application of hilbert-huang transform in processing projectile shock signal[C]//2009 international conference on information engineering and computer science. IEEE, 1–4

Li J, Liu C, Zeng Z et al (2015) GPR signal denoising and target extraction with the CEEMD method[J]. IEEE Geosci Remote Sens Lett 12(8):1615–1619

Li X, Li Z, Wang E et al (2016) Extraction of microseismic waveforms characteristics prior to rock burst using Hilbert-Huang transform[J]. Measurement 91:101–113

Li L, Wang F, Shang F et al (2017) Energy spectrum analysis of blast waves based on an improved Hilbert-Huang transform[J]. Shock Waves 27(3):487–494

Ma X, Zhou X, An FP (2020) Bi-dimensional empirical mode decomposition (BEMD) and the stopping criterion based on the number and change of extreme points. J Ambient Intell Hum Comput 11:623–633

Qian P, Jiang Y, Deng Z, Hu L, Sun S, Wang S, Muzic RF (2015) Cluster prototypes and fuzzy memberships jointly leveraged cross-domain maximum entropy clustering. IEEE Trans Cybern 46(1):181–193

Qian P, Jiang Y, Wang S, Su KH, Wang J, Hu L, Muzic RF (2016) Affinity and penalty jointly constrained spectral clustering with all-compatibility, flexibility, and robustness. IEEE Trans Neural Netw Learn Syst 28(5):1123–1138

Qian P, Zhao K, Jiang Y, Su KH, Deng Z, Wang S, Muzic RF (2017) Knowledge-leveraged transfer fuzzy C-means for texture image segmentation with self-adaptive cluster prototype matching. Knowl-Based Syst 130:33–50

Qian P, Zhou J, Jiang Y, Liang F, Zhao K, Wang S, Su K, Muzic RF Jr (2018a) Multi view maximum entropy clustering by jointly leveraging inter-view collaborations and intra-view-weighted attributes. IEEE Access 6:28594–28610

Qian P, Xi C, Xu M, Jiang Y, Su KH, Wang S, Muzic RF (2018b) SSC-EKE: semi-supervised classification with extensive knowledge exploitation. Inf Sci 422:51–76

Shucong L, Lina C, Lixin L (2016) Research on seismic signals denoising method based on multi-threshold wavelet packet[J]. Int J Sig Process Image Process Pattern Recognit 9(2):297–306

Wang D, Song L, Zhang Z (2010) A pressure measurement system based on stored measurement theory for explosion shock waves[C]//2010 International Symposium on Intelligent Signal Processing and Communication Systems. IEEE, 1–4

Wu Z, Huang NE (2009) Ensemble empirical mode decomposition: a noise-assisted data analysis method[J]. Adv Adapt Data Anal 1(01):1–41

Xia K, Yin H, Zhang Y (2019a) Deep semantic segmentation of kidney and space-occupying lesion area based on SCNN and resnet models combined with SIFT-flow algorithm. J Med Syst 43(1):2

Xia K, Yin H, Qian P, Jiang Y, Wang S (2019b) Liver semantic segmentation algorithm based on improved deep adversarial networks in combination of weighted loss function on abdominal CT images. IEEE Access 7:96349–96358

Xia K, Zhong X, Zhang L, Wang J (2019c) Optimization of diagnosis and treatment of chronic diseases based on association analysis under the background of regional integration. J Med Syst 43(3):1

Xu Q, Jin C (2003) Analysis of characteristic parameters in nonideal shock wave data: wavelet thresholds[C]//independent component analyses, wavelets, and neural networks. Int Soc Opt Photon 5102:354–359

Xu Y, Shen Q, Jin W et al (2020) Radial Hilbert transform for phase retrieval using two-wavelength three-frame phase-shifting interferometry[J]. Opt Lasers Eng 124:105846

Xue X, Zhou J, Xu Y et al (2015) An adaptively fast ensemble empirical mode decomposition method and its applications to rolling element bearing fault diagnosis[J]. Mech Syst Sig Process 62:444–459

Xue L, Zhou Y, Chen T, Luo X, Gu G (2017) Malton: towards on-device non-invasive mobile malware analysis for ART." In proceeding of USENIX security symposium (USENIX Security'17), pp. 289–306

Xue L, Qian C, Zhou H, Luo X, Zhou Y, Shao Y, Chan ATS (2018a) NDroid: toward tracking information flows across multiple android contexts. IEEE Trans Inform Forensics Secur (TIFS) 14(3):814–828

Xue L, Ma X, Luo X, Chan EWW, Miu TTN, Gu G (2018b) Linkscope: toward detecting target link flooding attacks. IEEE Trans Inform Forensics Secur (TIFS) 13(10):2423–2438

Yang H, Ning T, Zhang B et al (2017) An adaptive denoising fault feature extraction method based on ensemble empirical mode decomposition and the correlation coefficient[J]. Adv Mech Eng 9(4):1–9

Yao Z, Wang Z, Forrest JYL et al (2017) Empirical mode decomposition-adaptive least squares method for dynamic calibration of pressure sensors[J]. Meas Sci Technol 28(4):045010

Yeh JR, Shieh JS, Huang NE (2010) Complementary ensemble empirical mode decomposition: a novel noise enhanced data analysis method[J]. Adv Adapt Data Analy 2(02):135–156